

Generation of THz radiation at KEK LUCX facility

JAI Seminar: Introduction Seminar by Recently Started Research Staff

K. Lekomtsev on behalf of LUCX collaboration

Personal Introduction

Konstantin Lekomtsev

Currently: Marie – Curie research fellow at Royal Holloway University of London.

2012 – 2016: Postdoctoral researcher at High Energy Accelerator Research Organization (KEK), Tsukuba, Japan.

- Analytical studies and Simulations of the radiative phenomena in electron accelerators (Transition, Diffraction, Cherenkov, Smith-Purcell etc.).
- High power fs laser system tuning and maintenance, experimental studies at the Laser Undulator Compact X-ray facility (LUCX).
- etc.

2009 – 2012: Marie – Curie early stage researcher (PhD student) at Royal Holloway University of London

- Analytical studies of coherent Diffraction radiation.
- Experimental study at CLIC Test Facility 3 at CERN.
- etc.

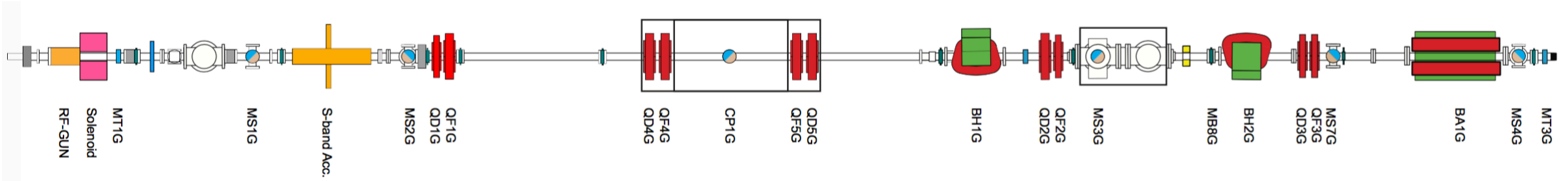
Earlier: National Research Nuclear University (Moscow Engineering Physics Institute)

- Master degree in Applied Mathematics.

Introduction

1. Overview of the LUCX facility.
 - a. Beam parameters.
 - b. Multi-bunch beam generation.
2. Monochromaticity of coherent THz Smith-Purcell radiation (SPR).
 - a. Brief theoretical background.
 - b. Particle In Cell simulations of SPR spectrum.
 - c. Discussion of experimental data.
3. Cherenkov Smith – Purcell radiation (ChSPR) from corrugated capillary.
 - a. Brief theoretical background and comparison with simulations.
 - b. Particle In Cell simulations of the radiation from multi-bunch beam and capillary with reflector.
 - c. Discussion of experimental data.

LUCX facility: Overview



- The Laser Undulator Compact X-ray facility (LUCX) is a multipurpose linear accelerator which was initially constructed as an RF gun test bench and later extended to facilitate Compton scattering and coherent radiation generation experiments.

“Femtosecond mode”

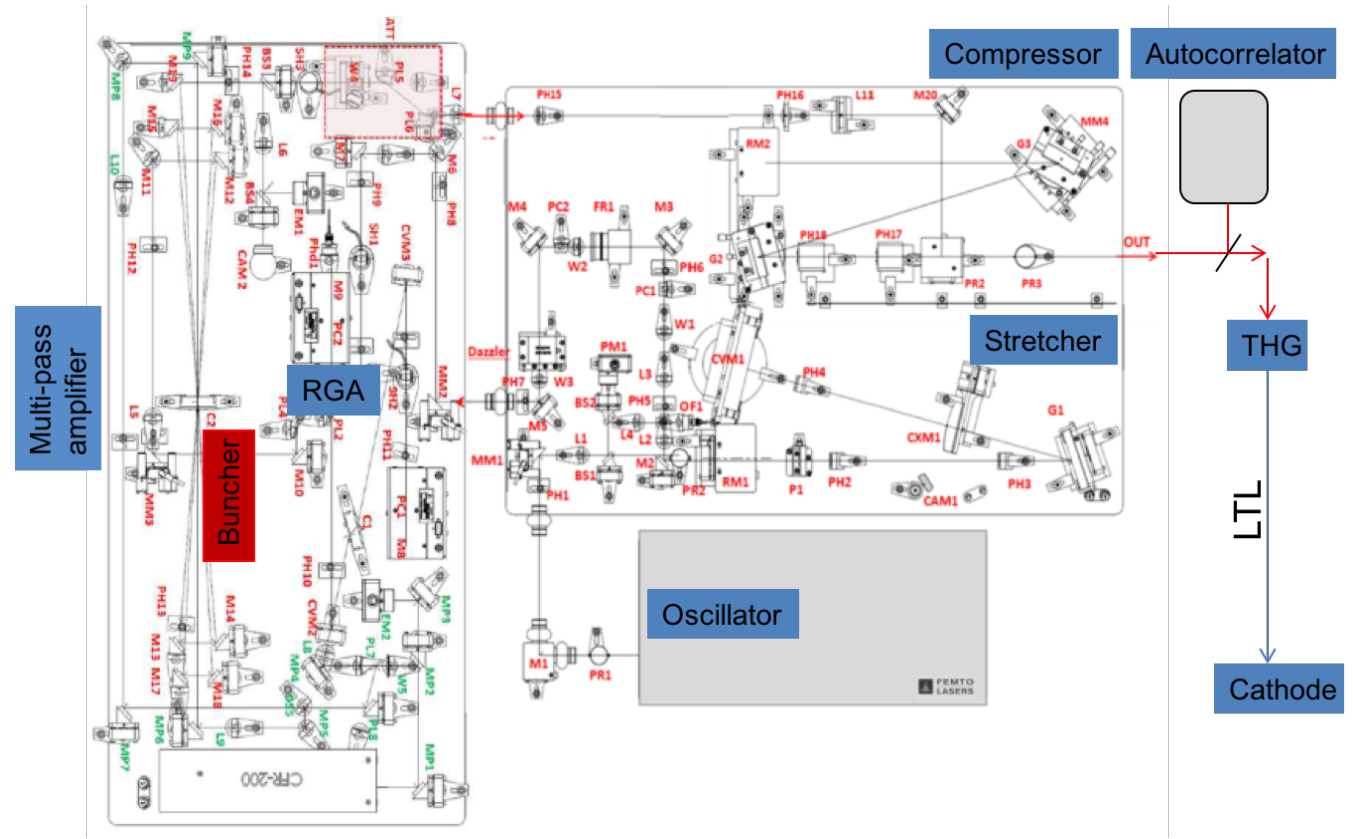
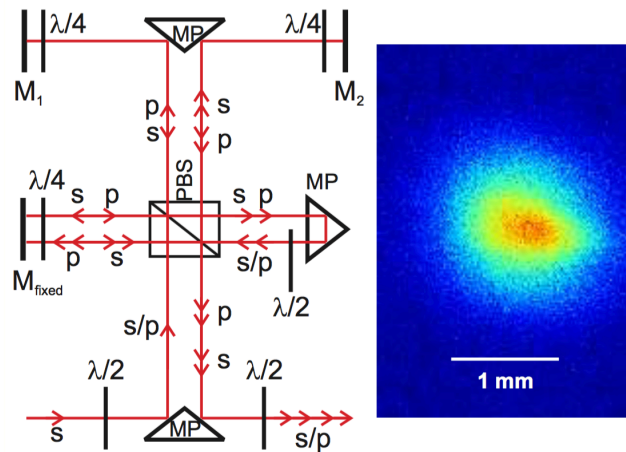
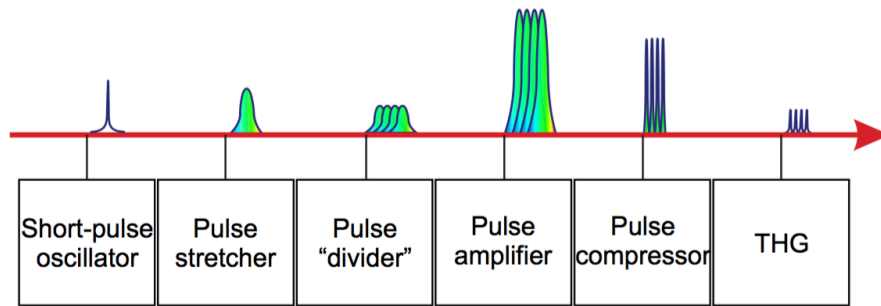
- Ti:Sa laser
- e-bunch RMS length ~ 100 fs
- e-bunch charge < 100 pC
- Single bunch train, Micro-bunching 4-16 (4 is confirmed)
- Typical Rep. rate 3.13 Hz
- Experiments: THz program

“Picosecond mode”

- Q-switch Nd:YAG laser
- e-bunch RMS length ~ 10 ps
- e-bunch charge < 0.5 nC
- Multi-bunch train 2- few 10^3
- Max Rep. rate 12.5 Hz
- Experiments: Compton, CDR

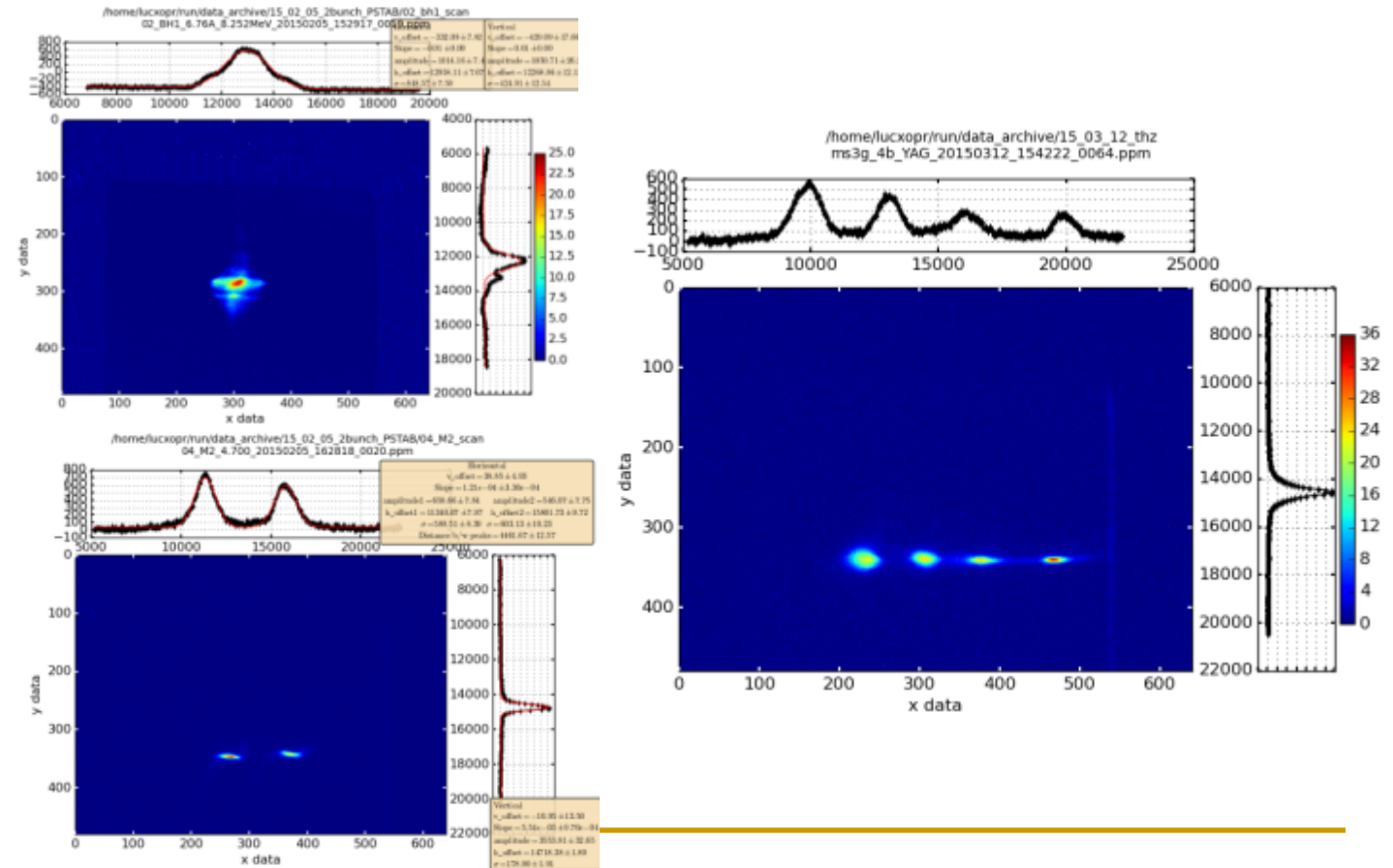
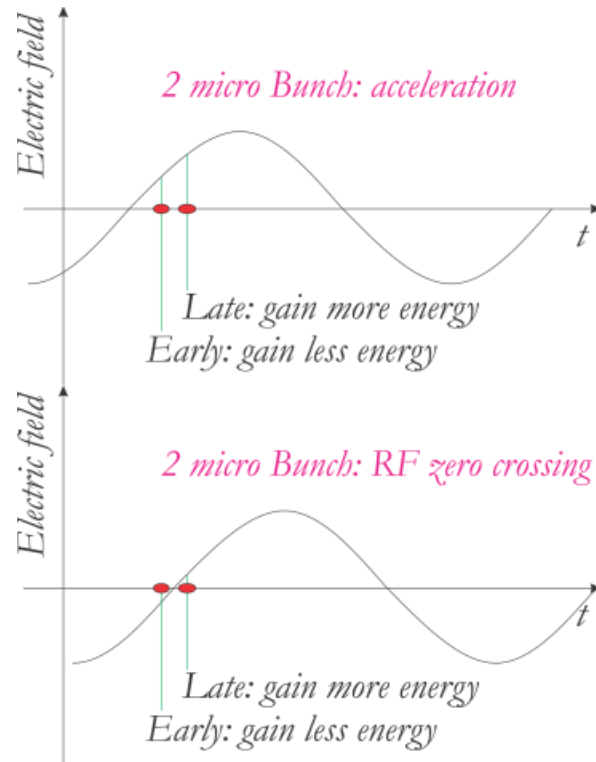
LUCX laser system

- Femtosecond duration electron bunches with THz repetition frequency illuminate a photocathode and an electron beam is generated on a single RF accelerating field cycle.
- Titanium – Sapphire “Chirped Pulse Amplification technique” laser system is used to generate a sequence of micro bunches.



Micro-bunch beam generation and characterization

- The RMS electron bunch length is measured by the [zero-phasing method](#) *. Time correlated momentum deviation imposed on the bunch if we operate at the zero crossing of the accelerating wave.
- The beam is then dispersed by a dipole magnet *BH1G* so that the different time slices of the electron bunch are projected onto a scintillating YAG screen at different horizontal positions, and thus beam [image on the screen shows the intensity distribution of the electron bunch along its temporal profile](#).
- [The correlation](#) of the RF phase with the YAG beam image shift [is measured](#).
- [The linear correlation of this approximation](#) gives the scale of the horizontal image size in RF degrees, which can be [recalculated to time scale](#).



* D.X. Wang et al, Phys. Rev. E 57, 2283 (1998).

Monochromaticity of SPR

Smith-Purcell radiation appears when charged particles move above and parallel to a diffraction grating. Spectral lines positions are defined by the dispersion relation *:

$$\lambda_k = \frac{d}{k} \left(\frac{1}{\beta} - \cos\theta \right); \quad (1)$$

where λ_k is the wavelength of the resonance order k , d is the grating period, β is the particle in the units of the speed of light, and θ is the observation angle.

The spectral-angular distribution of the coherent SPR ** produced from grating with finite number of periods N :

$$\frac{d^2W}{d\nu d\Omega} = \frac{d^2W_0}{d\nu d\Omega} \frac{\sin^2[N\varphi]}{\sin^2[\varphi]} (N_e + N_e(N_e - 1)F); \quad (2)$$

$\varphi = d \frac{\pi\nu}{c} (\beta^{-1} - \cos\theta)$ - phase associated with strips periodicity, $\frac{d^2W_0}{d\nu d\Omega}$ is the spectral angular distribution from a single grating period, ν is radiation frequency, N is the number of grating periods, N_e is the bunch population, and F is the bunch form-factor.

From (2), if FWHM is taken as an absolute spectral line width, the monochromaticity is defined as:

$$\frac{\Delta\lambda}{\lambda} = \frac{0.89}{kN}. \quad (3)$$

* S.J. Smith and E.M. Purcell, Visible light from localized surface charges moving across a grating, Phys. Rev. 92, 1069 (1953).

** A.P. Potylitsyn et al., Diffraction Radiation from Relativistic Particles, Springer (2010).

Monochromaticity of SPR

Measurements limitations:

The width of SPR spectral lines can become larger if they are measured by the detector placed in the so called “pre-wave zone”. If the grating to detector distance is L , then the far-field zone (or wave zone) condition is determined by *:

$$L \gg L_{ff} = kN^2 d(1 + \cos\theta).$$

Monochromaticity of the radiation generated from an infinite grating ($N \rightarrow \infty$) and measured with a finite aperture detector $\Delta\theta$:

$$\frac{\Delta\lambda}{\lambda} = \frac{\sin\theta}{\frac{1}{\beta} - \cos\theta} \Delta\theta.$$

Assuming that the real line shape $\delta\lambda_r$ and the spectrometer resolution $\delta\lambda_{sp}$ can be approximated by a Gaussian distribution, the FWHM of the measured line:

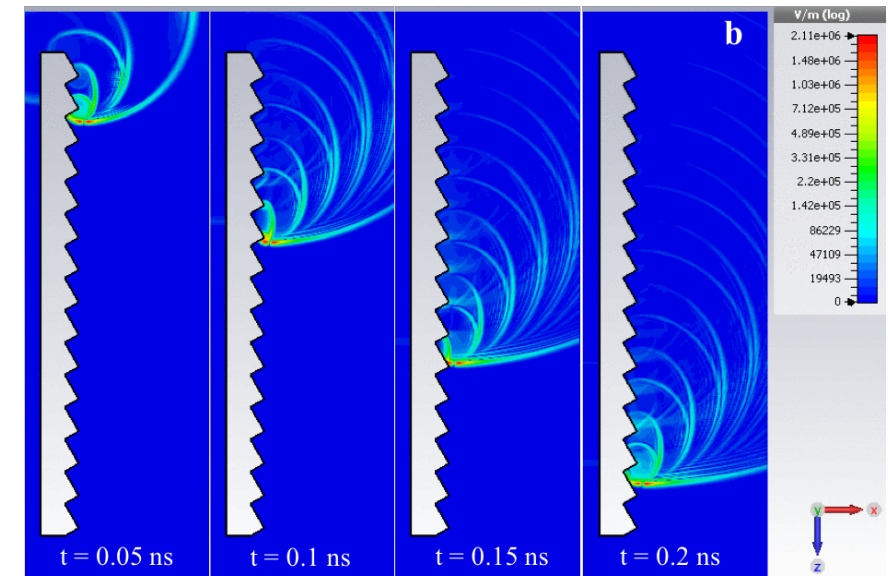
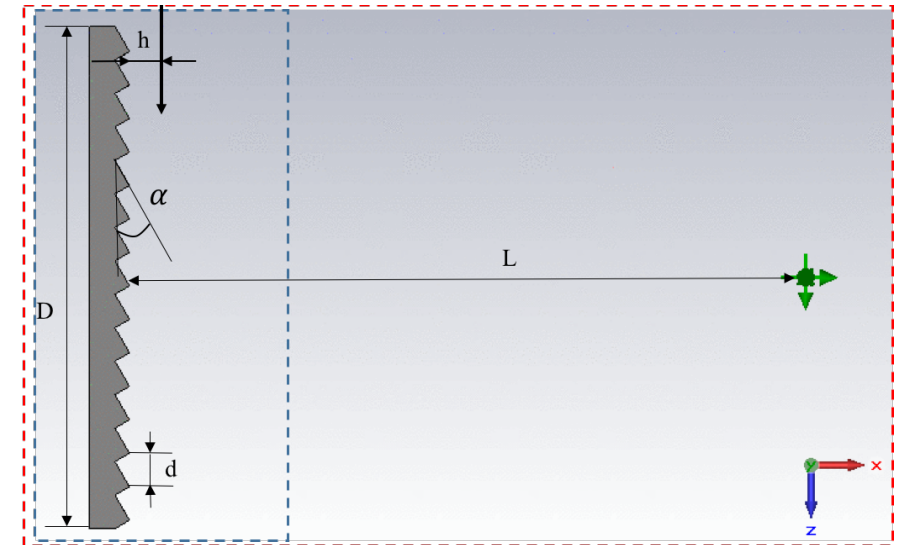
$$\delta\lambda = \sqrt{\delta\lambda_r^2 + \delta\lambda_{sp}^2}.$$

* D.V. Karlovets and A.P. Potylitsyn, JETP Letters 84, 489 (2006).

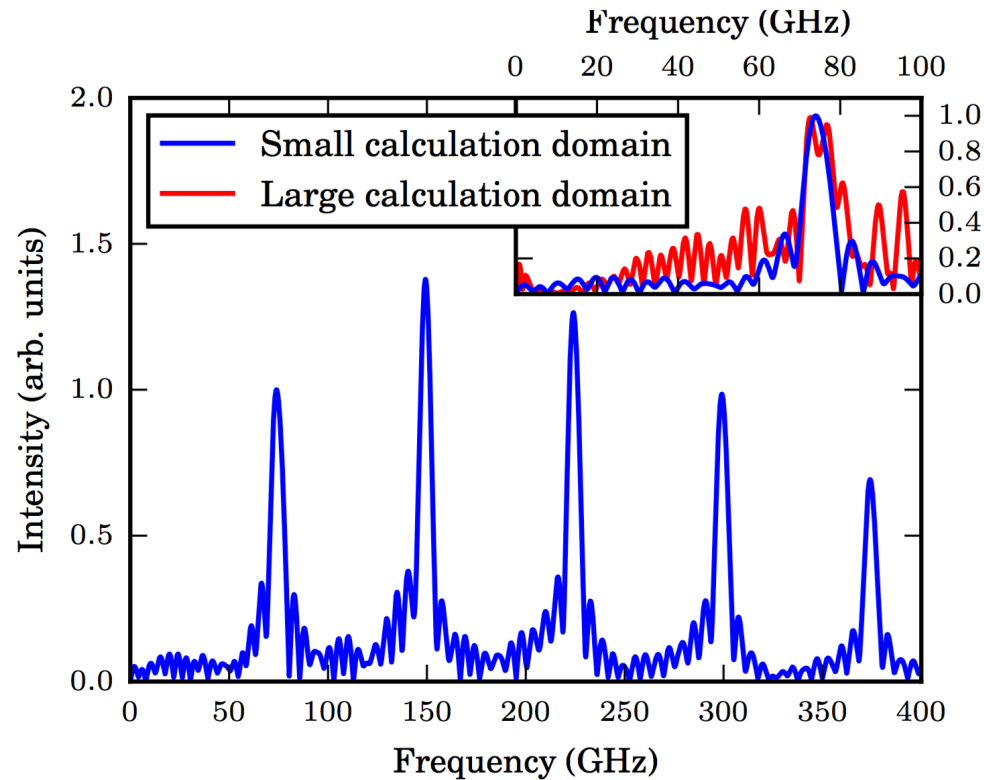
Particle in Cell simulations (SPR)

- Simulations were performed in [CST Particle Studio, Particle In Cell Solver](#).
- Considered [two calculation domains](#) in order to show the influence of the pre-wave zone effect for the first diffraction order of SPR.
- SPR spectrum obtained by [recording electric field components as functions of time](#) and then by [performing Fourier transform](#) of the time dependence of the dominant component.

Simulation parameter	Value
L	500 mm
D	60 mm
h	0.6 mm
d	4 mm
α	30 deg.
Bunch length	0.5 ps
Bunch transverse size	250 μm
Beam energy	8 MeV



Particle in Cell simulations (SPR)

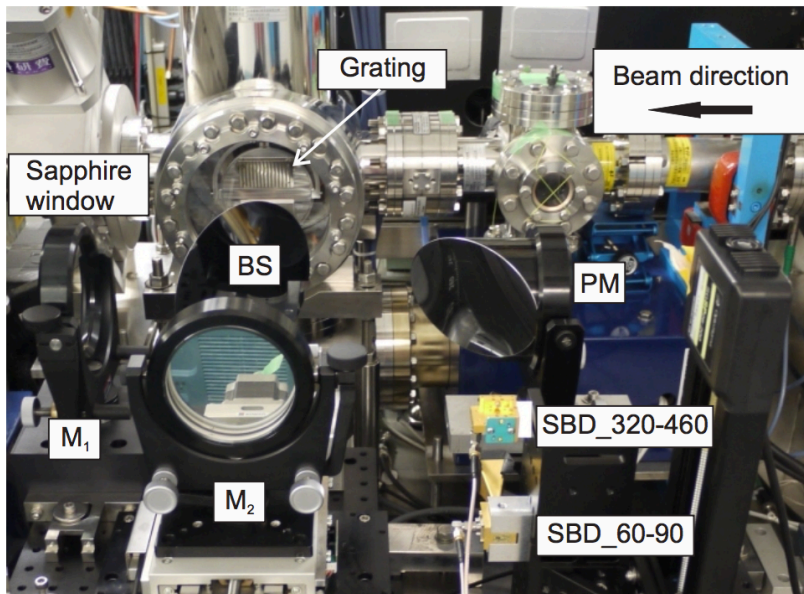
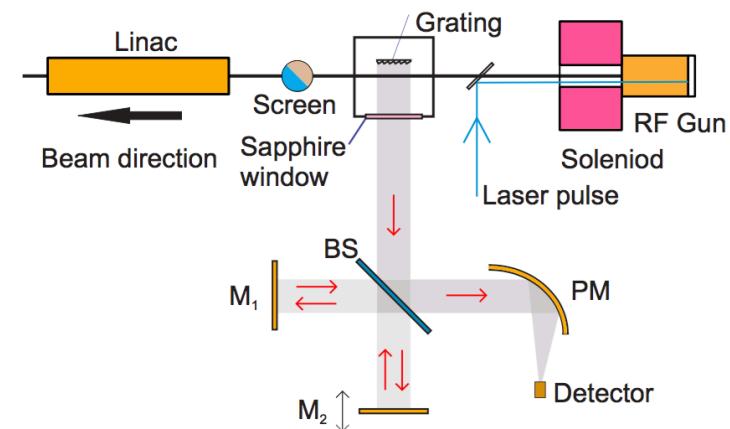


Comparison of the SPR spectral line widths:

k	Theory	Simulations
1	5.9%	10.3%
2	3.0%	4%
3	2.0%	2.9%
4	1.5%	2.4%
5	1.2%	1.9%

- Both the simulation and the theory show that higher order spectral lines become more monochromatic.
- When comparing the line widths for the theory and the simulation, it is important to remember that the theory was developed for $N \rightarrow \infty$ and not taking into account real shape of the grating.

Experimental study (SPR)



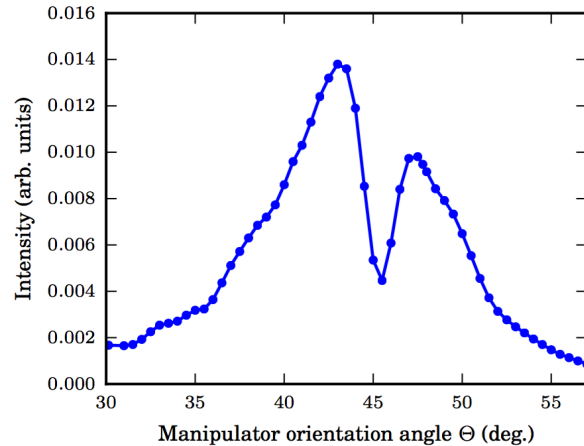
- Vacuum window: 12 mm thick 2 deg. wedged sapphire, with effective aperture of 145 mm.
- 5-axis manipulator system was installed on the top of the vacuum chamber. Used for fine adjustment of the grating positions in 3 orthogonal directions and also for the control for the 2 rotational angles.
- The grating was aligned with respect to the electron beam using the forward bremsstrahlung appearing due to direct interaction of the electron beam with the target material.

Parameter	Value
Beam energy	8 MeV
Charge per bunch	25 pC
Bunch length	0.5 ps
Transverse size	$230 \times 230 \mu\text{m}$
Repetition rate, max	12.5 train/s
Normalized emittance, type	$4.7 \times 6.5 \text{ mm mrad}$

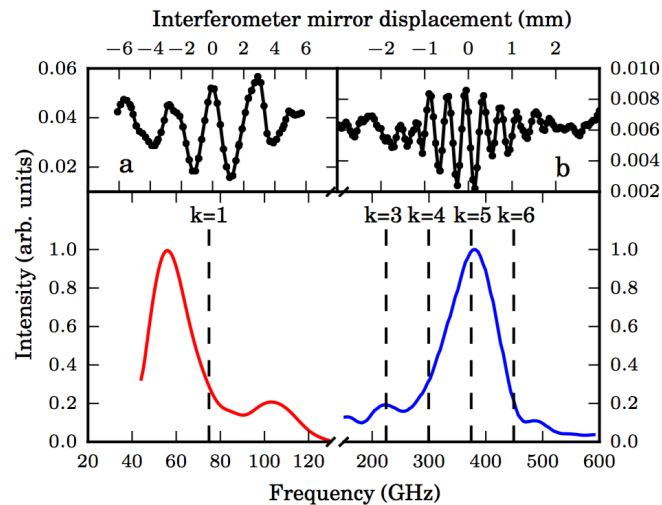
Parameter	SBD 60-90 GHz	SBD 320-460 GHz
Frequency range	60 – 90 GHz	320 – 460 GHz
Wavelength range	3.3 – 5.0 mm	0.94 – 0.65 mm
Response time	~ 250 ps	sub-ns
Antenna gain	24 dB	25 dB
Input aperture	$30 \times 23 \text{ mm}$	$4 \times 4 \text{ mm}$
Video sensitivity	20 V/W	1250 V/W

Experimental study (SPR)

Transition Radiation angular scan using SBD 320 - 460



Transition Radiation spectral measurements:



SBD 60 – 90 GHz
SBD 320 – 460 GHz

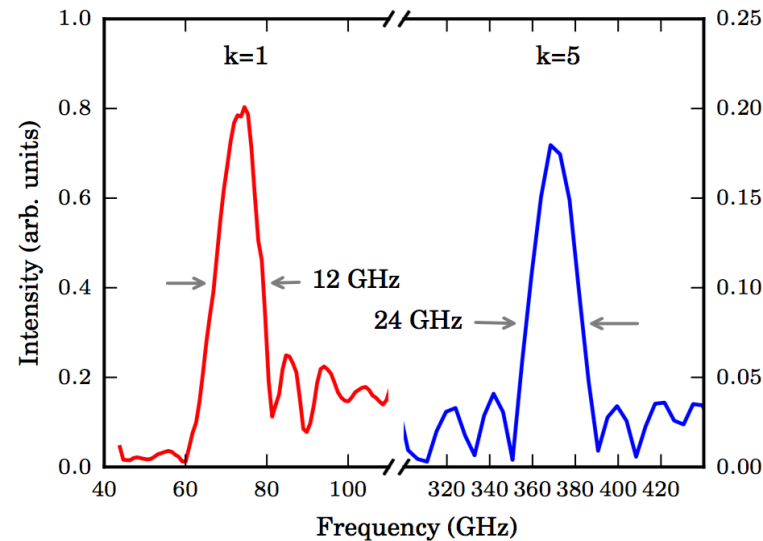
Measured normalized Transition Radiation spectrum can be used as spectral efficiency of the entire measurement system, including:

- ✓ spectral transmission efficiency of the vacuum window,
- ✓ detector wavelength efficiency,
- ✓ splitter efficiency,
- ✓ reflection characteristics of the mirrors and absorption in air.

Spectral resolution of Fourier spectrometer: $\delta\lambda$ defined as FWHM of the spectral peak from a monochromatic source:

$$\frac{\delta\lambda}{\lambda} = 1.21 \frac{\lambda}{2L_{int}}$$

where L_{int} is the interferometer maximum optical path difference from zero position.



Applying this criterion to the interferograms, the spectrometer resolution:

$$\frac{\delta\lambda_1}{\lambda_1} = 15\%; \frac{\delta\lambda_5}{\lambda_5} = 6\%$$

The measured peaks FWHM:

$$\frac{\delta\lambda_1^m}{\lambda_1} = 16\%; \frac{\delta\lambda_5^m}{\lambda_5} = 6.1\%$$

Theory and simulation of THz radiation from corrugated channel

Spectral – angular distribution * of the radiation generated as a result of the point like electron passing through corrugated channel in infinite dielectric ($R \rightarrow \infty$):

$$\frac{d^2 W(\mathbf{n}, \omega)}{d\Omega d\hbar\omega} = \frac{\alpha}{(2\pi)^2} \frac{|\varepsilon(\omega) - 1|^2}{\sqrt{\varepsilon(\omega)}} \frac{1}{(1 + \gamma^2 \beta^2 \varepsilon(\omega) \sin^2 \theta)^2 \varphi^2} \frac{\sin^2(k\varphi d N/2)}{\sin^2(k\varphi d/2)} \times$$

$$\times |[\mathbf{n}, \mathbf{e}_z] \{ (e^{-ik\varphi l} - 1)(F_1(r_1) - F_1(R)) + (e^{-ik\varphi d} - e^{-ik\varphi l})(F_1(r_2) - F_1(R)) \} +$$

$$+ \gamma[\mathbf{n}, \mathbf{e}_\perp] \{ (e^{-ik\varphi l} - 1)(F_2(r_1) - F_2(R)) + (e^{-ik\varphi d} - e^{-ik\varphi l})(F_2(r_2) - F_2(R)) \} |^2$$

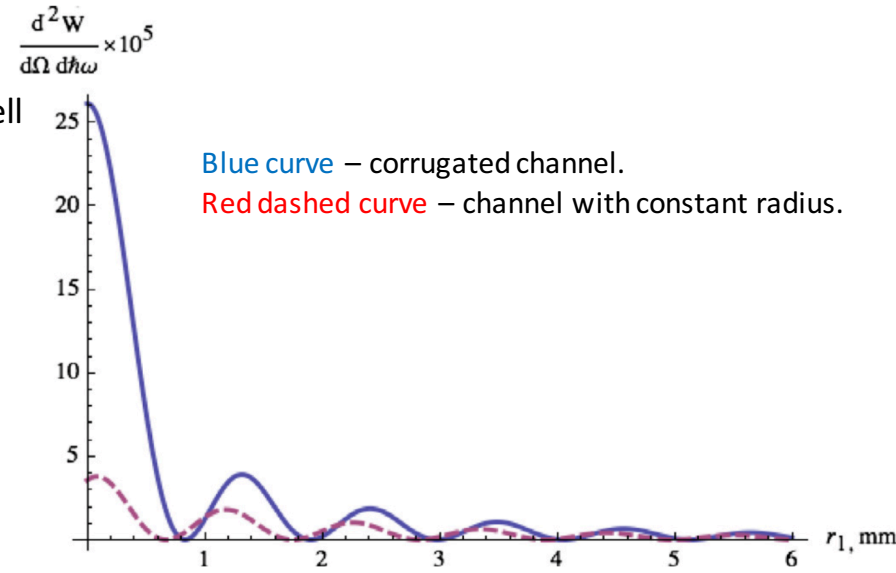
$$F_1(r) = -(kr \sin \theta) J_1(kr \sin \theta) K_0\left(\frac{kr}{\gamma\beta\sqrt{\varepsilon}}\right) + J_0(kr \sin \theta) \frac{kr}{\gamma\beta\sqrt{\varepsilon}} K_1\left(\frac{kr}{\gamma\beta\sqrt{\varepsilon}}\right)$$

$$F_2(r) = (kr \sin \theta) J_0(kr \sin \theta) K_1\left(\frac{kr}{\gamma\beta\sqrt{\varepsilon}}\right) + J_1(kr \sin \theta) \frac{kr}{\gamma\beta\sqrt{\varepsilon}} K_0\left(\frac{kr}{\gamma\beta\sqrt{\varepsilon}}\right)$$

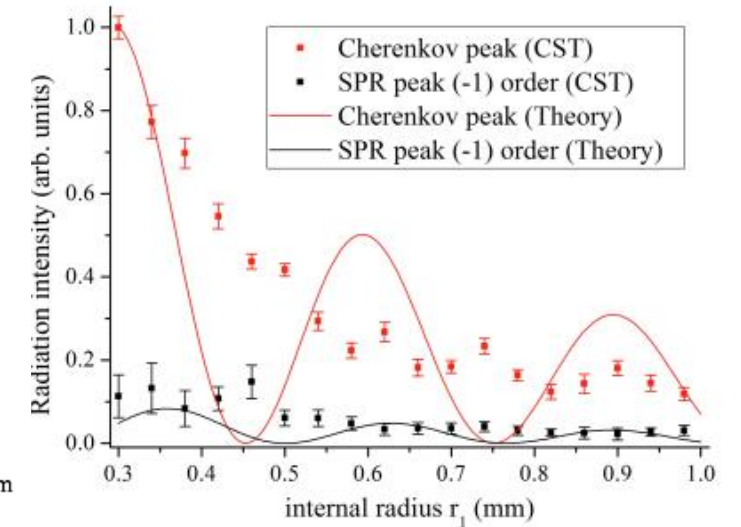
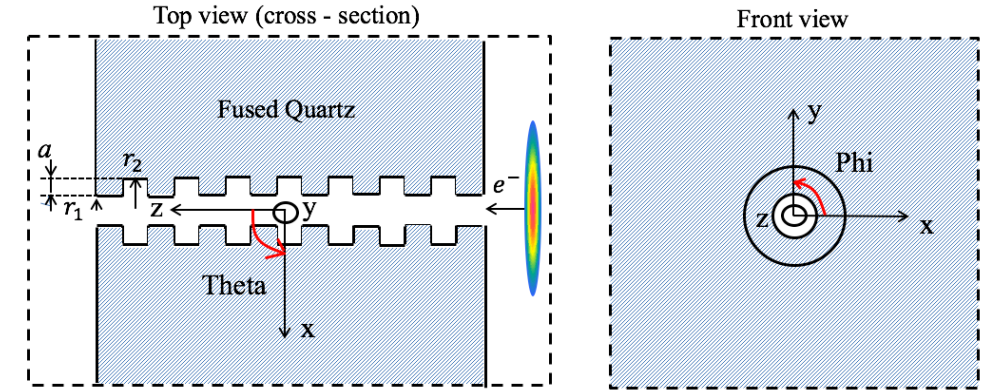
The diffraction orders of Cherenkov and Smith-Purcell radiation peaks satisfy the dispersion relation:

$$\cos(\theta) = \frac{2\pi m}{kd} + \frac{1}{\beta\sqrt{\varepsilon(\omega)}};$$

where θ is polar angle, β is the electron speed in terms of the speed of light, k is the wavenumber in dielectric, d is the corrugation period, m is a diffraction order, $\varepsilon(\omega)$ is dielectric permittivity as a function of frequency.



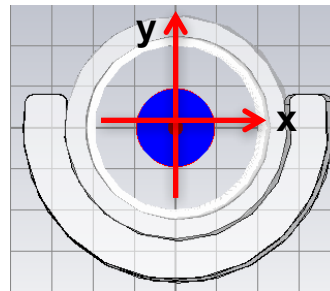
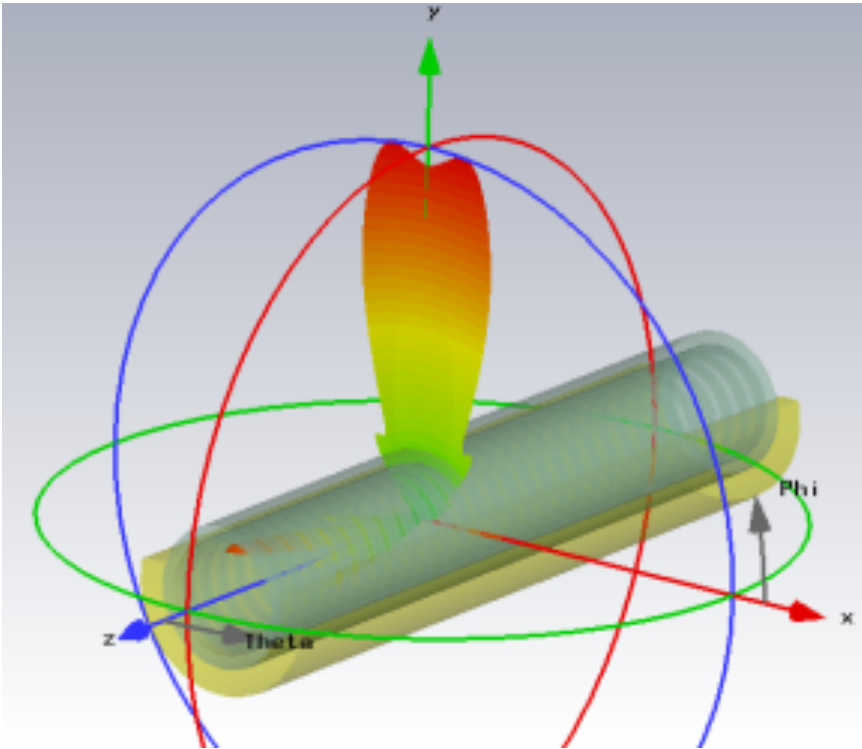
CST Particle In Cell simulation:



* A.A. Ponomarenko et. al, Terahertz radiation from electrons moving through a waveguide with variable radius, based on Smith-Purcell and Cherenkov mechanisms, NIMB 309, 223 (2013).

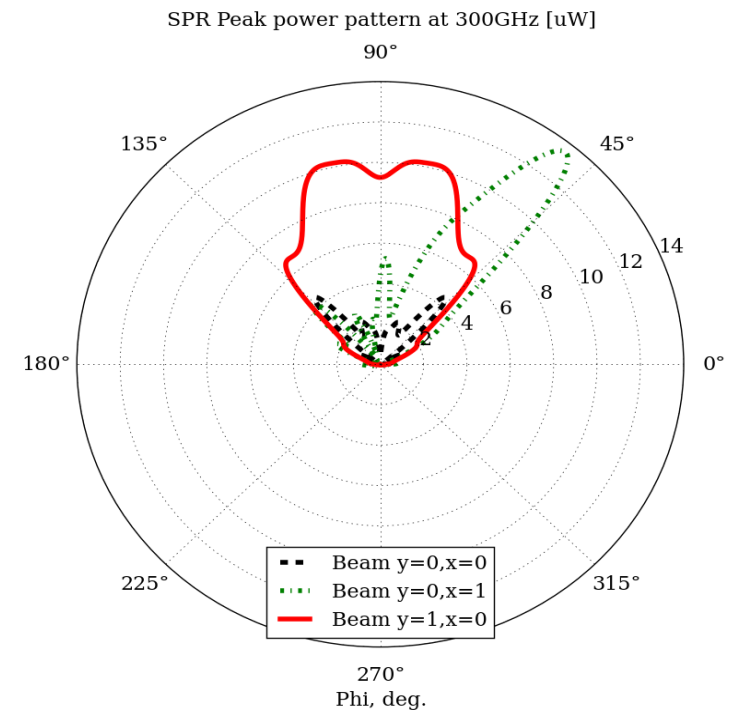
PIC simulations (ChSPR)

- 3D power pattern and the corresponding azimuthal cross-sections ($\theta = 90$ deg.) for the radiation at 300 GHz for the off-central beam propagation $x=0$, $y=1$ mm.
- Cherenkov radiation is reflected by the outside boundaries of the corrugated capillary and directed at small angles $\theta \approx 10$ deg.

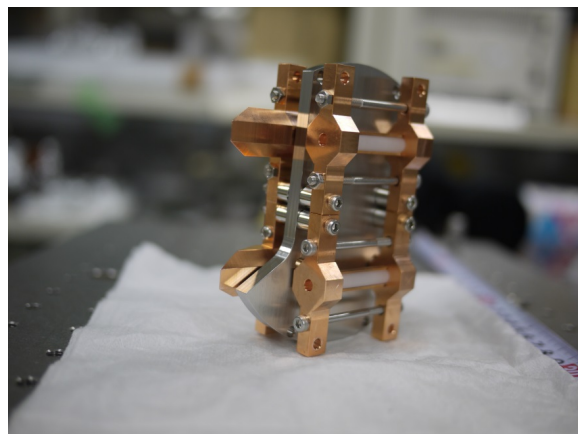
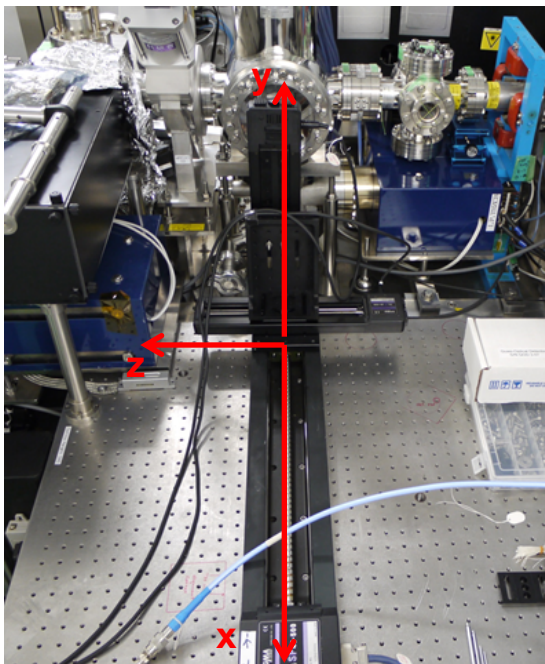


$$P_{peak} = \frac{P(\omega)}{\Delta t},$$

$\Delta t = 0.13$ ns
(simulation time)



Experiment (ChSPR)

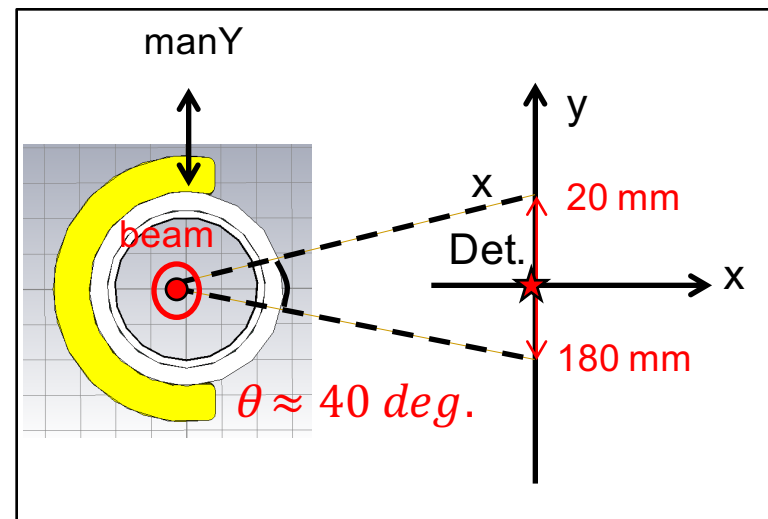
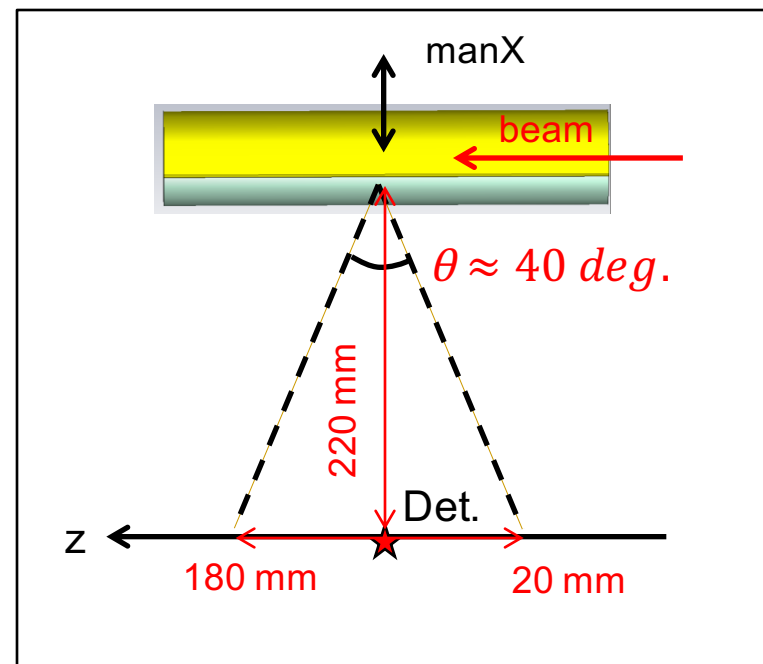
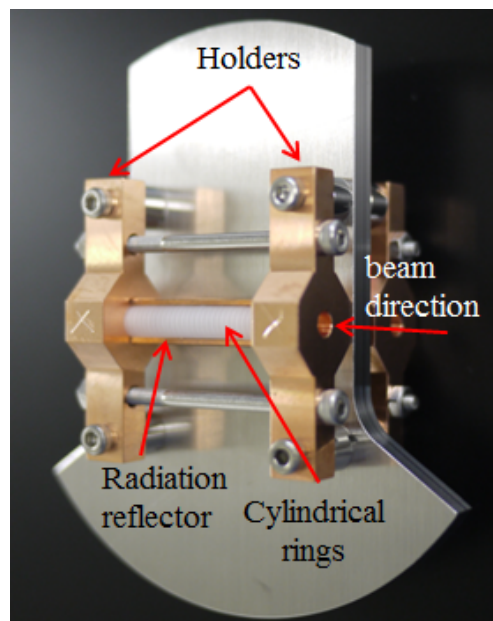


Bunch size:
 $200 \times 200 \mu\text{m}$

Bunch charge:
1 bunch 25 pC

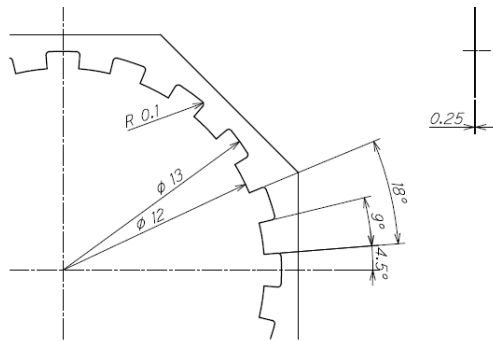
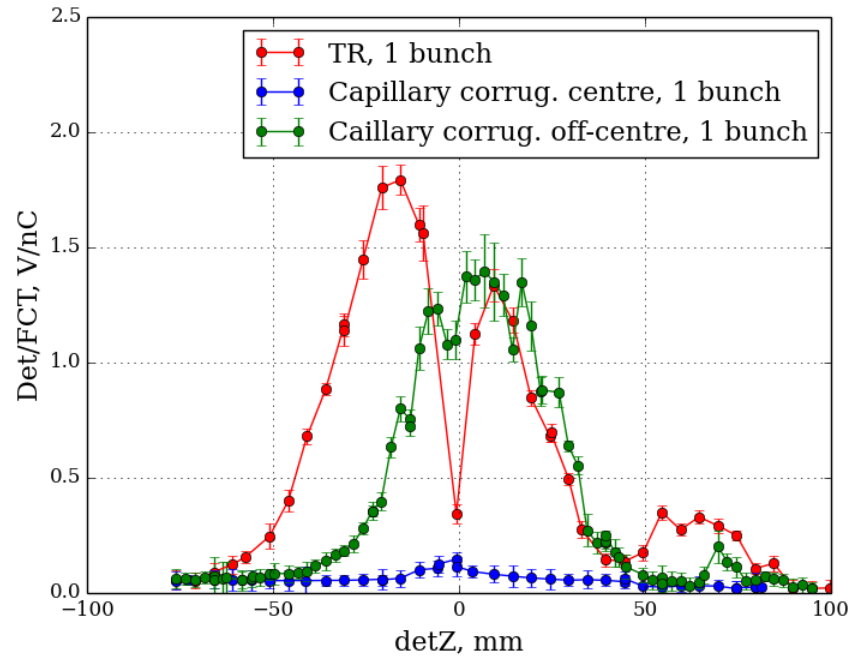
Detector:
SBD 320 – 460 GHz

Quartz vacuum window:
100 mm (effective diameter)

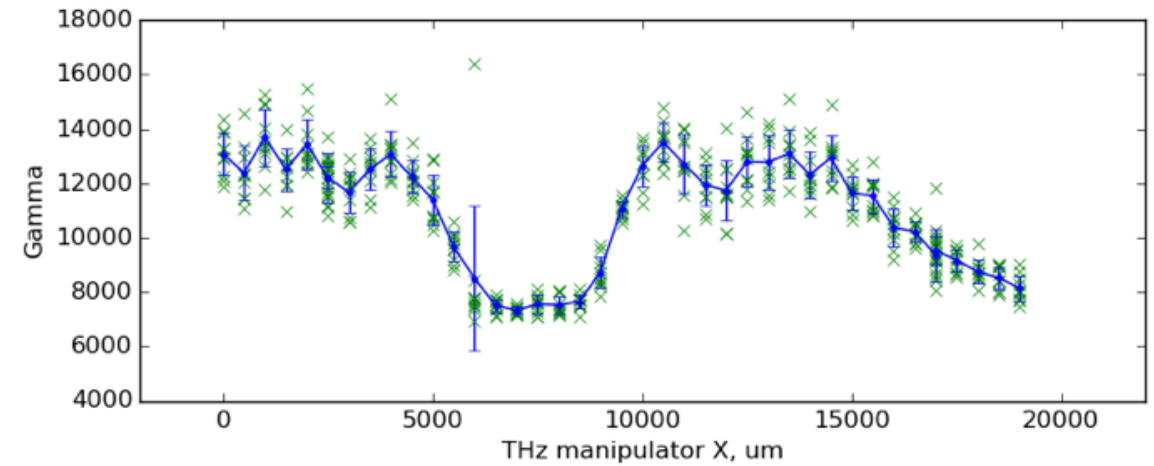
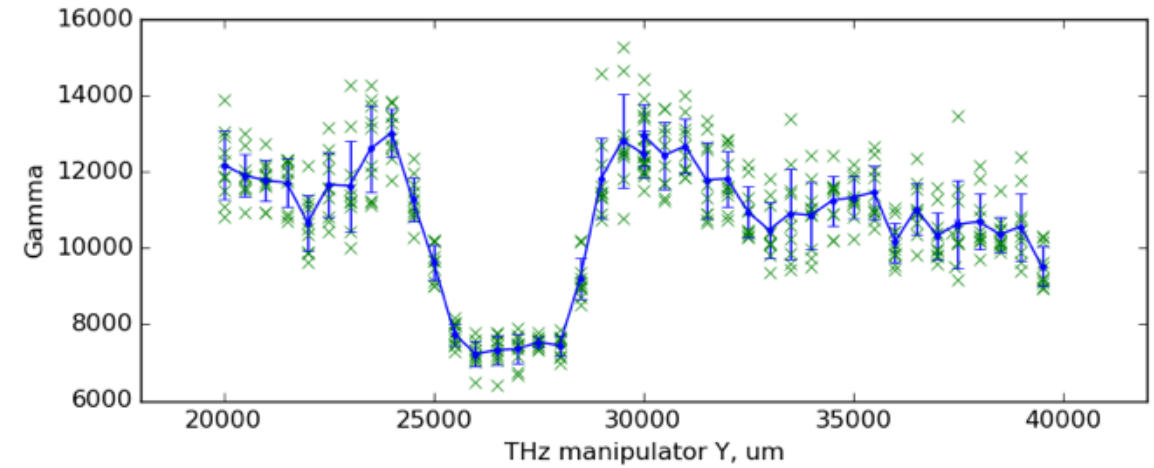


Experiment (ChSPR)

Cross-check with Transition radiation:

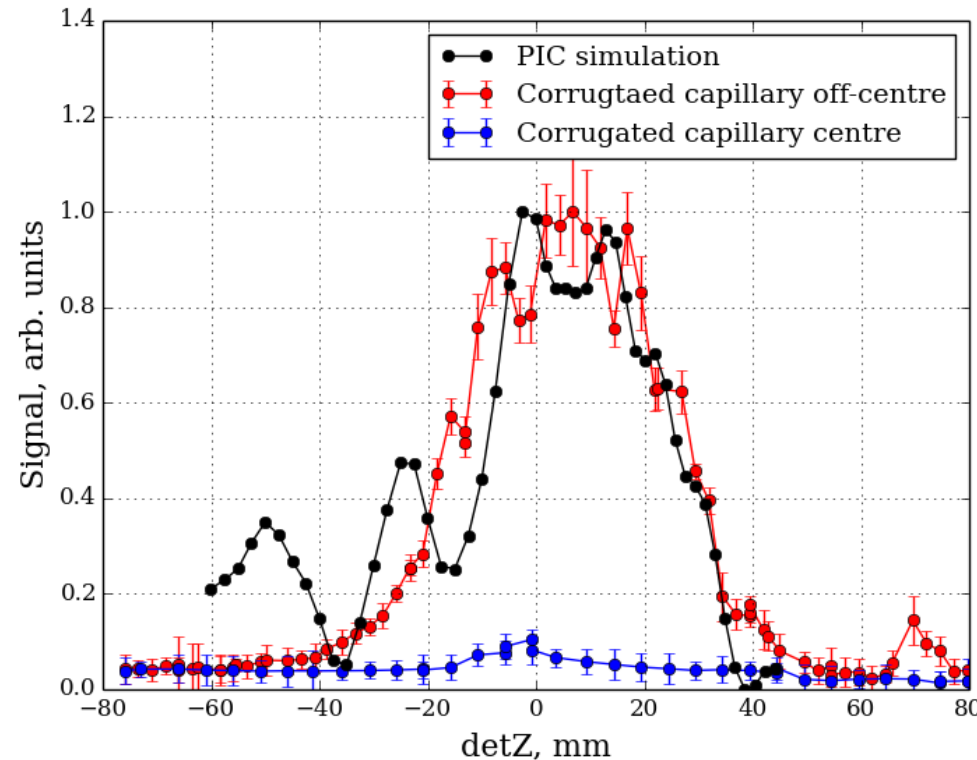
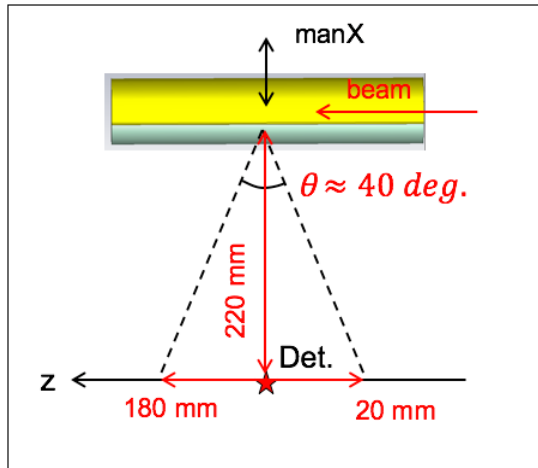


Positioning of the capillaries with respect to the beam
(bremsstrahlung, appearing due to direct interaction of the
electron beam with the target material):



Experiment (ChSPR)

The polar distribution of the radiation:



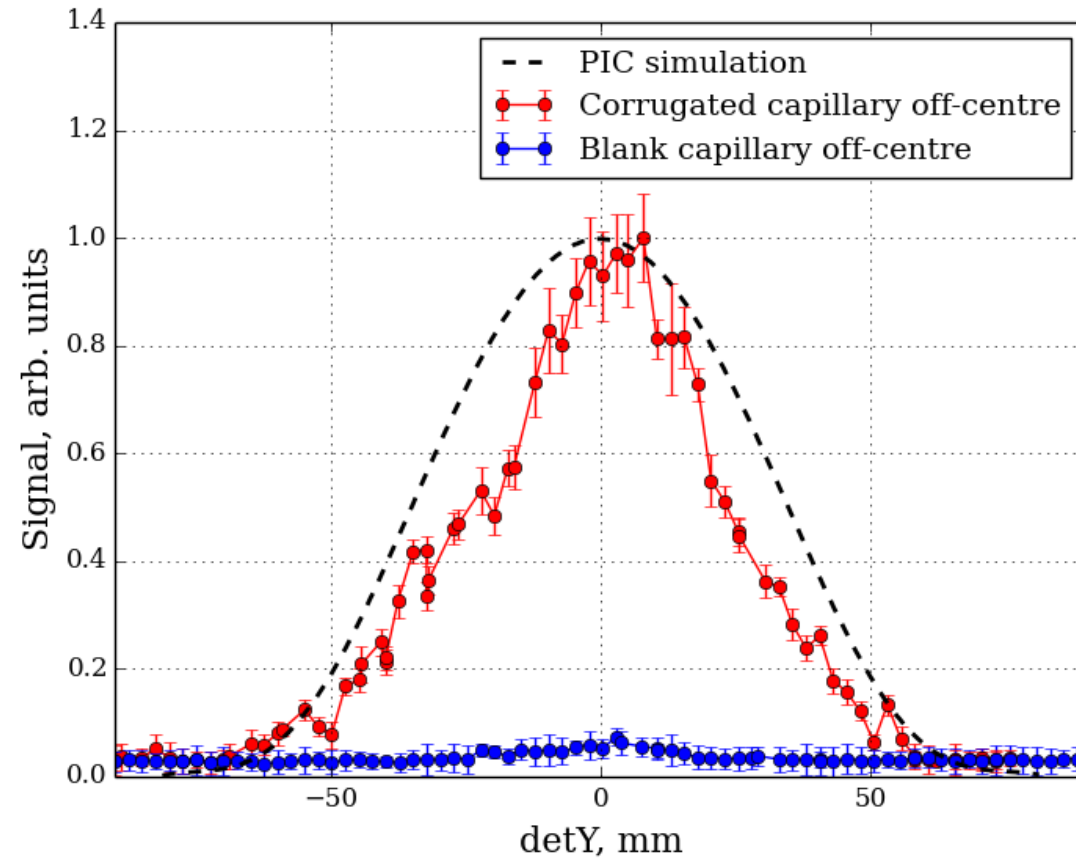
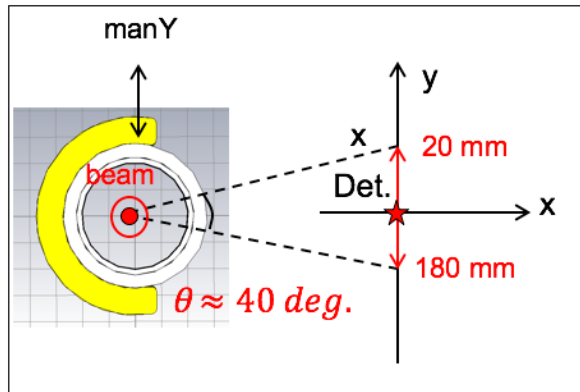
- The simulated geometry was identical to the realistic one with the exception of holders, which were not taken into account in the simulations.
- The beam parameters were chosen to be the same as during the time of the experiment, and the beam was moving at 0.6 mm from the corrugation to allow for 3σ beam – corrugation separation.
- The power distribution was obtained by, first, calculating the power spectrum of emitted radiation in the frequency range 240 – 360 GHz. The radiation directivity pattern for each frequency was calculated as well, hence it was possible to convert power spectrum into the power distribution at the detector locations on the translation stage.
- After the converted power distribution was obtained, the beam contribution in the power spectrum was subtracted.
- The power spectrum of the radiation emitted through the surface of the outside boundary A of the calculation domain during the simulation time Δt was calculated as:

$$P(\omega) = \left| \int_0^{\Delta t} \oint \mathbf{S}(\omega) * \mathbf{n} dA dt \right|;$$

where $\mathbf{S}(\omega)$ is the Poynting vector, \mathbf{n} is a unity vector in the outward normal direction from the boundary A of the calculation domain.

Experiment (ChSPR)

The azimuthal distribution of the radiation:



- Azimuthal distribution of the radiation was simulated using the [far-field monitor of CST Particle Studio](#), which extrapolates the electric field values at the border of the calculation domain to obtain the electric fields in the far-field (distances $\gg \gamma^2 \lambda$) at a single frequency.
- According to the dispersion relation: $\cos(\theta) = \frac{2\pi m}{kd} + \frac{1}{\beta\sqrt{\epsilon(\omega)}}$ the frequency at $\theta = 90\text{deg.}$ ($\det Z = 0$) is 300 GHz ($\lambda = 1\text{mm}$).
- The red curve: [measurement of the azimuthal distribution of the radiation at 300GHz](#).

Overview and outlook

- The main objective of the SPR study was to demonstrate the feasibility to generate SPR with monochromaticity better than 1 - 2%, by choosing a higher diffraction order and relatively small number of periods (in the order of 10).
- The measurements were limited by several factors, including the resolution of the spectrometer, the quality of its alignment, angular acceptance of the detector. All of these factors contribute to the widening of the measured spectral lines.
- Further monochromaticity improvements are expected if a multi-bunch beam is used.

- The objectives of the ChSPR study were to cross-check the radiation with other well known radiation mechanism (TR), to study the effect of corrugation and measure the radiation distributions.
- Measured 10-fold increase of the radiation intensity for the corrugate capillary in comparison to the blank capillary.
- Confirmed that the maximum of the radiation intensity is achieved for the off-central beam propagation.
- The composite design of the corrugated capillary allows for flexibility to easily change the geometry, which can be very useful for a variety of studies including radiation generation, beam energy and charge modulation etc.

Marie Skłodowska-Curie Horizon 2020 project

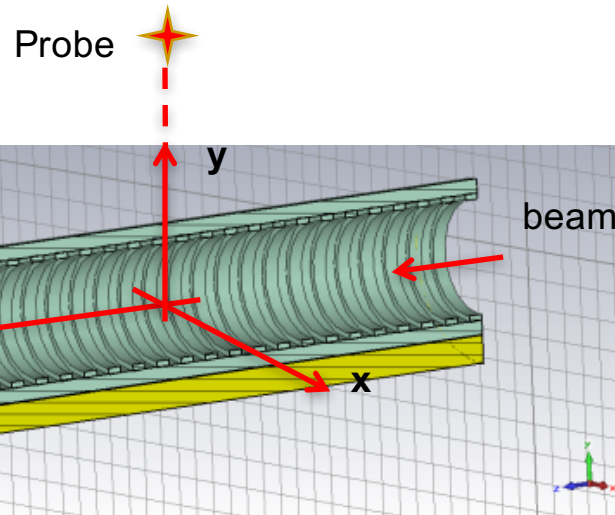
Research objectives:

- to investigate Cherenkov and Smith - Purcell mechanisms for THz radiation generation using EM simulation tools and propose the most efficient target configuration and observation geometry;
- to manufacture a radiation source that provides high peak power levels and based on a compact linear accelerator technology with fs-duration beam;
- to evaluate the possible applications of the investigated radiation mechanisms for beam position and bunch length diagnostics;
- To expand research interests in the directions which allow for effective skills and knowledge transfer (dielectric wake-field acceleration, accelerator-scale wake-field simulations, evaluation of positive and negative effects of wake-fields in accelerator).
- to provide the knowledge exchange between the partner organizations and other interested parties via seminars, satellite and progress meetings, conferences and workshops;
- to improve the public awareness about the ongoing research via outreach activities;
- to further develop project management skills (financial, workflow, deliverables planning etc.)

Acknowledgements:

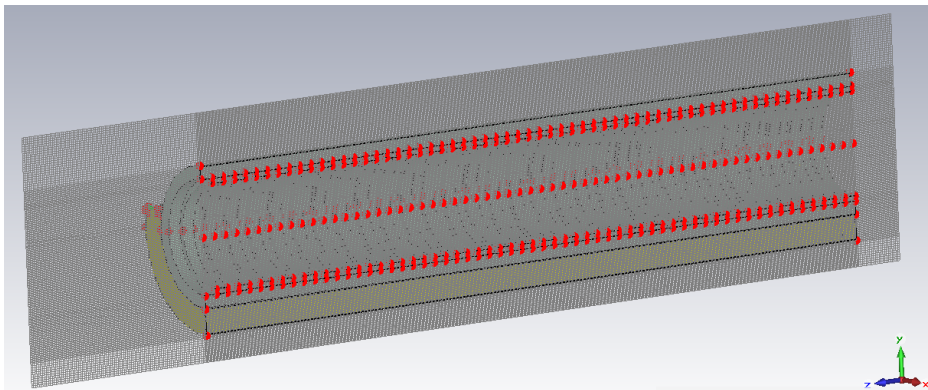
This project has received funding from the European Union's Horizon 2020 research and innovation programme under the Marie Skłodowska-Curie grant agreement No 655179.

PIC simulations (capillary with reflector)



Simulation geometry (general view):

- Electric field probe is located outside of the calculation domain;
- The field values at the probe location are obtained based on the extrapolation of the field values at the border of the calculation domain *.

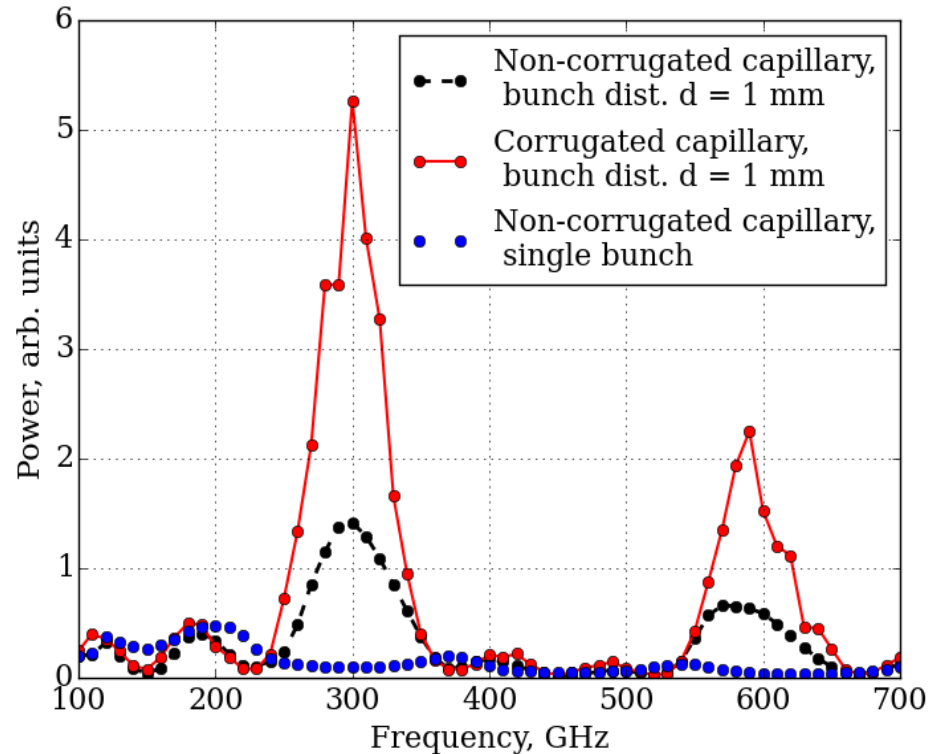


Simulation geometry (mesh view in Oyz plane):

Parameter	Value
beam Lorentz - factor, γ	16
frequency	up to 700 GHz
bunch length, σ_{long}	0.03 mm
bunch transverse size, σ_{transv}	0.3 mm
micro-bunch charge	0.1 nC
N of micro-bunches	4
distance between micro-bunches	variable (0.25 – 1 mm)
capillary material	Fused quartz
holder material	Copper
number of periods	30
cylindrical ring width, l	0.5 mm
corrugation period, $2l$	1 mm
groove depth, $r_2 - r_1$	0.2 mm
internal radius, r_1	2 mm
outer radius, r_3	2.7 mm

* Yee K S, Ingham D and Shlager K 1991 Time-Domain Extrapolation to the far field based on FDTD calculations *IEEE Trans. of Ant. and Prop.* **39** 410

PIC simulations (capillary with reflector)



Resonant condition:

bunch distance = corrugation period

The power radiated through the surface of the outside boundary A of the calculation domain during the simulation time Δt at each frequency is given by the following expression:

$$P(\omega) = \left| \int_0^{\Delta t} \oint \mathbf{S}(\omega) * \mathbf{n} dA dt \right|;$$

where $\mathbf{S}(\omega)$ is the Poynting vector, \mathbf{n} is a unity vector in the outward normal direction from the boundary A of the calculation domain.

Single bunch:

relatively flat response at all frequencies.

Blank capillary:

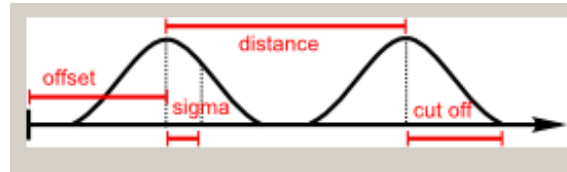
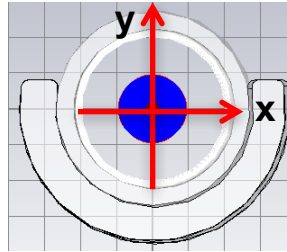
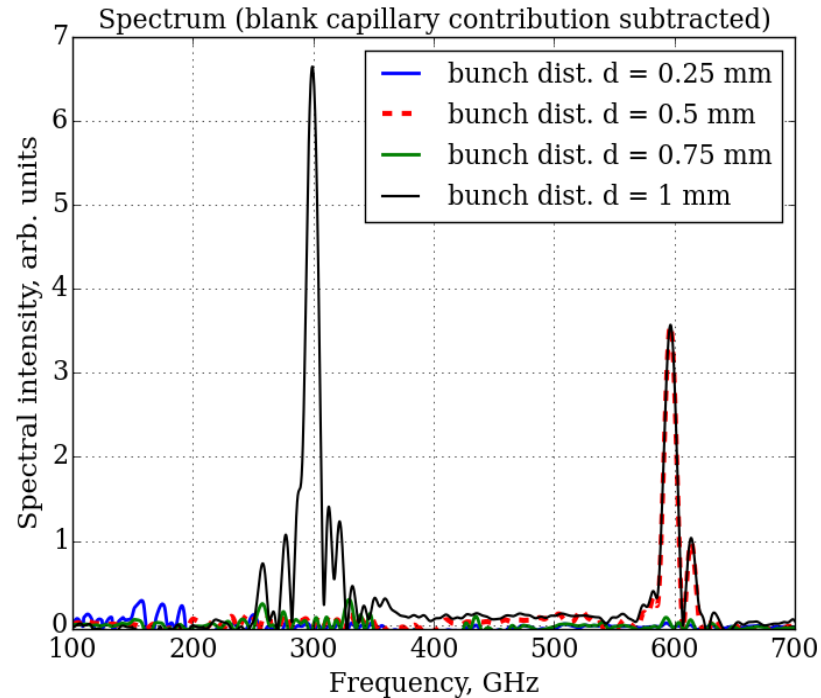
power spectral modulation due to Cherenkov radiation.

Corrugated capillary:

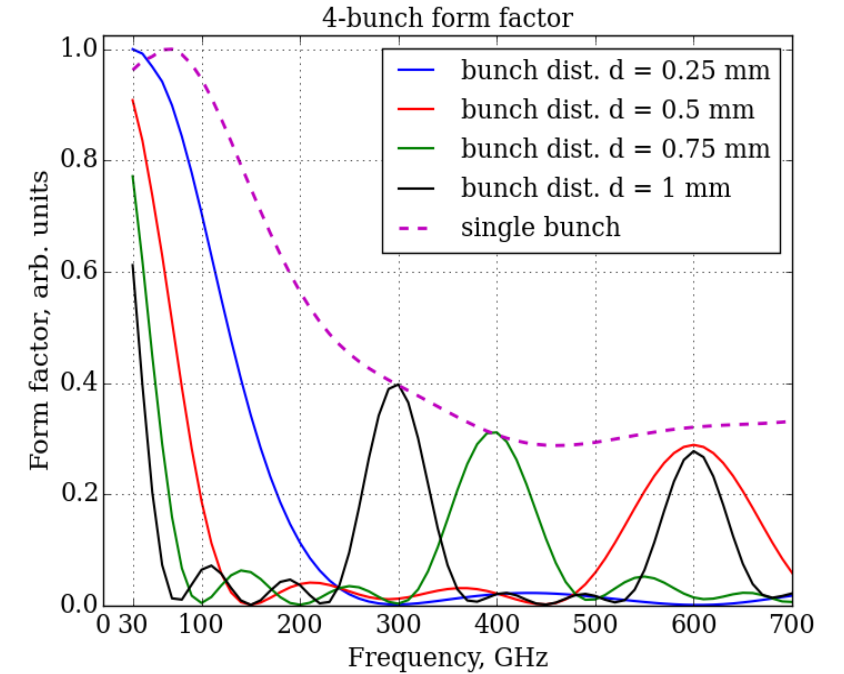
even larger spectral modulation if the distance between bunches is equal to the corrugation period.

PIC simulations (capillary with reflector)

Beam position: $x = 0$ mm, $y = 1$ mm



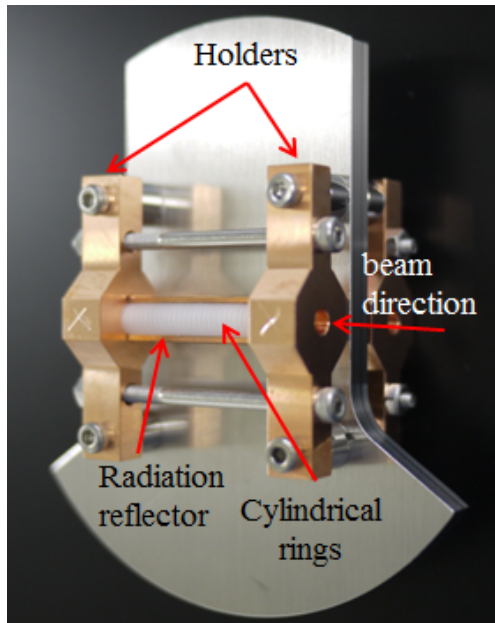
Form-factors of four bunches with different bunch spacing, and the form factor of a single bunch:



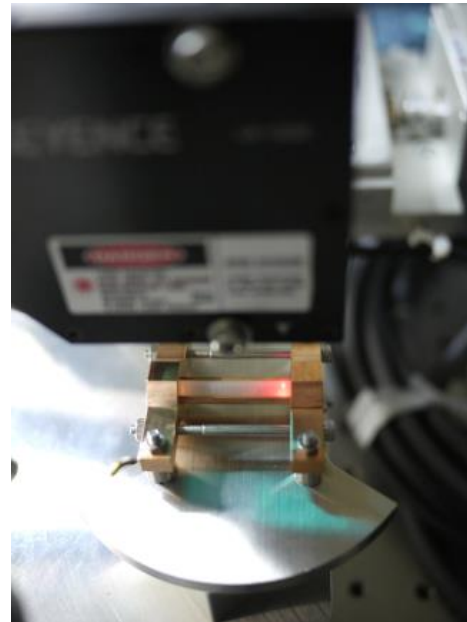
Spectral modulation of the radiation depends on the periodicity of the corrugation as well as the distance between bunches.

Assembly of the capillary with holders

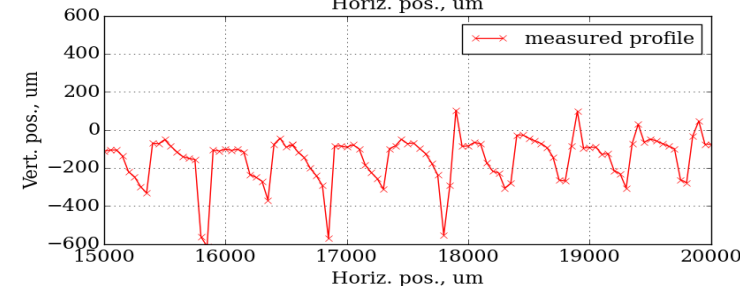
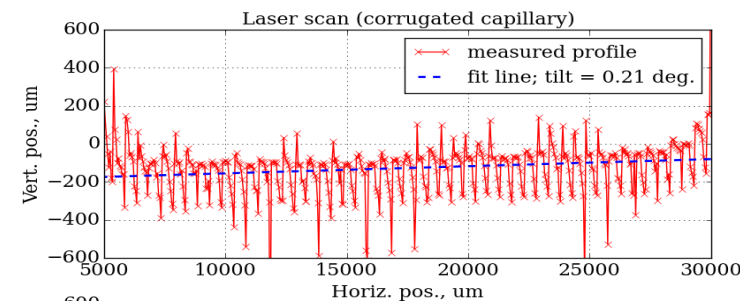
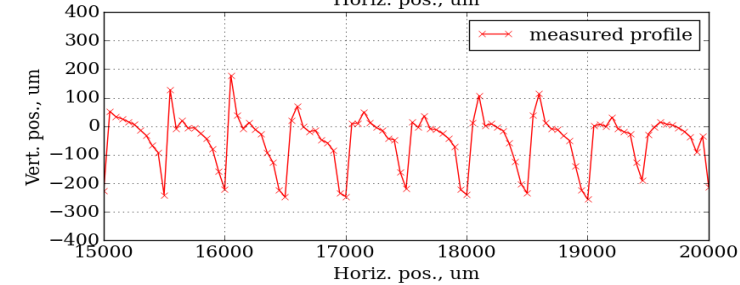
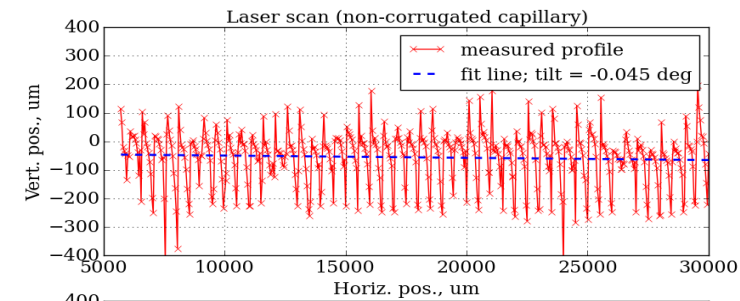
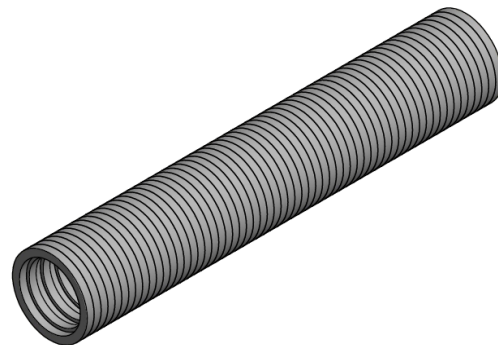
Capillary with holders and radiation reflector assembled on the base plate:



Laser scans were performed on the outside surface of the capillary installed in the holders:

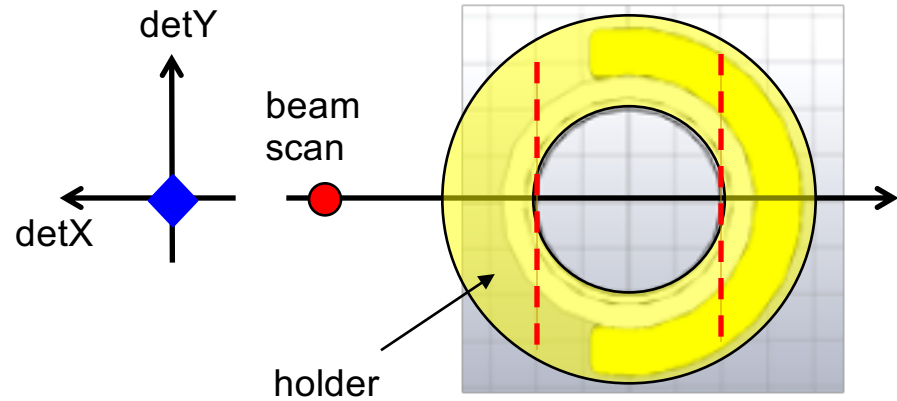


Both corrugated and blank capillaries are constructed as sets of cylindrical rings:



- Laser beam scanned along the outer surface of corrugated and blank capillaries.
- Light reflected from the surface detected by an array detector and the vertical offset of the laser beam recorder.
- As a result obtained the vertical offset as a function of the horizontal travel range.

Experiment (capillary with reflector)



Target – beam separation and the corresponding radiation yield:

